

Quasi-solid-state dye-sensitized solar cells: Pt and PEDOT:PSS counter electrodes applied to gel electrolyte assemblies

Matteo Biancardo*, Keld West, Frederik C. Krebs

The Danish Polymer Centre, RISØ National Laboratory, P.O. Box 49, DK-4000 Roskilde, Denmark

Received 21 August 2006; received in revised form 19 October 2006; accepted 2 November 2006

Available online 9 November 2006

Abstract

In this paper we present an attempt to substitute liquid electrolyte (LC) dye-sensitized solar cells (DSSCs) by quasi-solid-state constructions (SC) for semi-transparency application adopting organic/inorganic gels in combination with standard (Pt based) and alternative (PEDOT:PSS based) counter electrodes. Gel polymer electrolytes are prepared by incorporating a liquid electrolyte into a polymer matrix such as polymethylmethacrylate (PMMA) using propylene carbonate (PC) as gelling solvent. SC employing gel electrolytes with a high content in PC have been shown to exhibit increased lifetime up to 70 h under A.M. 1.5 irradiation. Counter electrodes were prepared by an airbrushing and tape casting technique of Pt salt solutions or by spin coating of commercial PEDOT:PSS solution. PEDOT:PSS counter electrodes were found to show similar I_3^-/I^- catalytic activities to Pt based counter electrodes and the best SC obtained gave a short circuit current of 2 mA cm^{-2} and an open circuit voltage of 625 mV.

© 2006 Elsevier B.V. All rights reserved.

Keywords: Quasi-solid-state solar cells; Polymer electrolytes; Sensitization; TiO_2

1. Introduction

Since the original report of the dye-sensitized solar cell by O'Regan and Grätzel in 1991 [1], almost 15 years of research has led to the development of efficient and low cost LCs at the laboratory level [2]. Problems related to reliability, durability and engineering in construction of integrated products remain crucial and have to be solved before commercialization can be envisaged.

In our previous work [3] we addressed long-term stability problems due to electrolyte leakage in LCs by producing SC modules. These modules employed PMMA-based gel electrolytes and aimed at increasing stability and transparency of DSSCs rather than the cell efficiency. In this paper, we introduce new gel recipes with higher content in low boiling point solvents to improve the SC lifetime and we address potential optimizations at the counter electrodes.

The most common approach to fabricate solid-state DSSCs is by using p-type semiconductors as hole transport materials

[4–6], followed by the use of ionic liquids [7–9] and polymer electrolytes [10–23].

The use of polymers in DSSCs have been developing in three directions: towards the production of flexible solar cells substituting the glass substrates with plastic substrates [10]; to avoid the presence of liquid electrolyte by employing gel [11–16] or polymer electrolytes [17–19]; or to find a replacement for the expensive Pt based counter electrode, such as PEDOT [20–23]. In this paper we present a quasi-solid-state construction combining two of these approaches. The liquid electrolyte was replaced by a gel electrolyte and the Pt counter electrode was replaced by PEDOT:PSS, which was produced by spin coating a commercial aqueous dispersion onto fluorine doped tin oxide (FTO) substrates.

Quasi-solid-state DSSCs employs gel electrolytes consisting of a polymer network swollen with a solvent to perform the function of shuttling the generated positive charge away from the light absorbing sensitizer on the semiconductor surface to the counter electrode [24]. The use of polymer gel electrolytes can take advantage of the fact that gel electrolytes have been widely studied as a conductive material for batteries and fuel cells [25] and therefore present a solid reference for potential industrial applications.

* Corresponding author. Tel.: +45 46774718; fax: +45 46774791.
E-mail address: matteo.biancardo@risoe.dk (M. Biancardo).

Within the wide variety of polymers employed as electrolytes two are the most diffused: polyethylene oxide (PEO) and PMMA [26]. PEO based electrolytes are the earliest and most extensively studied system for Li-batteries [26] as well as for solid-state DSSCs [24]. These systems usually refer to solvent-free PEO/salt complexes in which the ionic conduction mechanism is intimately associated with the local segmental motion of the polymer (ionic conductivity increases with increasing chain mobility). Typically solvent-free PEO–salt complexes exhibit conductivity in the range from 10^{-8} to 10^{-4} S cm $^{-1}$ at temperature between 40 and 100 °C, which excludes practical applications at ambient temperature. To obtain better conductivities at room temperature is necessary to use, blends [27], copolymers, or cross-linked networks [28]. PMMA-based electrolytes were firstly used as gelatinization agent in 1985 with a reported conductivity of 10^{-3} S cm $^{-1}$ at 25 °C [29]. In combination with PC as plasticizer, PMMA produces homogeneous and transparent gels that have both the cohesive properties of solids and the diffusive transport properties of liquids. In particular, the conductivities of these gels remains very close to that of a liquid electrolyte since PMMA acts primarily as a “stiffener” and fasts ion transport through a continuous conduction path of PC molecules [29]. For their characteristics of transparency and conductivity PMMA gel electrolytes were preferred to PEO pure polymer electrolytes in this study.

The remarkable properties of PEDOT as a conductive polymer have been intensively studied since its discovery in 1988 [30]. In DSSCs this polymer has been principally used as a hole transport material (HTM) [31–33] for solid-state solar cells, despite the interesting new findings questioning the need of HTMs in DSSCs [34]. As a counter electrode PEDOT has been studied doped with toluene sulphonic acid (TOSH) [23] and doped with polystyrenesulphonate (PSS) [21] in liquid and gel electrolyte assemblies. Yanagida and coworkers [21], reported a study on the charge transfer resistance and cyclic voltammetry in liquid environments and observed that PEDOT:TOSH have a higher I_3^-/I^- catalytic activity than the corresponding PSS doped PEDOT. However, Hayase and coworkers [22] discovered that a combination of conductive polymers and PEDOT:PSS counter electrodes gave photoenergy conversions higher than DSSCs equipped with conventional Pt counter electrodes.

The use of Pt counter electrodes in LCs or SCs is necessary to reduce the overpotential for reduction of the redox species I_3^- to I^- and therefore returning the mediator to its reduced state closing the circuit initiated by the charge injection into the semiconductor conduction band. Despite their high catalytic activity, conventional Pt counter electrodes are not optimal due to the high cost of the metal employed and to the airbrushing technique that increases the number and the complexity of the production steps. Several techniques have been used to produce Pt counter electrodes, namely, e-beam evaporation, sputtering, thermal decomposition of H_2PtCl_6 [35] and electrochemical deposition [36]. Few groups have used chemical approaches using colloidal preparation that provides electrodes by self-assembly [37] or by producing screen printable paste [38,39].

In this context, we firstly explored a tape casting technique for the Pt deposition. Finally we substituted the Pt metal with PEDOT:PSS as counter electrode, which have been shown to retain good catalytic activity in the regeneration process of the I_3^-/I^- redox couple [40] and finding that in a quasi-solid-state construction its catalytic activity is comparable to that of Pt.

2. Experimental

2.1. DSSCs preparation

DSSCs were realized on F-doped tin oxide (FTO) glass substrates (18 Ω /square, 3.0 mm thickness, supplied by Bley Glas ApS (DK)).

TiO $_2$ compact (TiO $_2$ comp) anatase film (0.1 μ m) were produced by spin coating 1 ml of a solution of Ti(IV)-isopropoxide (10 mL) and acetylacetone (7 mL) in ethanol (52 mL) at 2100–2200 rpm for 200 s followed by a sintering step at 500 °C for 30 min. A cleaning step employing sonication in acetone and iso-propanol of the FTO substrate was required before the spin coating step to ensure good adherence onto the glass substrate.

PEDOT:PSS layers were realized by spin coating (2000 rpm, 300 s) a microfiltered (1 μ m) 1.3 wt.% water dispersion (PEDOT 0.5 wt.%, PSS 0.8 wt.%, Aldrich) followed by a mild annealing process (20 min, 110 °C).

TiO $_2$ nanocrystalline (4 μ m film) and airbrushed Pt counter electrodes were deposited as reported previously [3].

The counter electrodes were prepared following different procedures.

Pt001, Pt counter electrodes (1 Ω /square) were prepared by airbrushing a fresh solution of H_2PtCl_6 (5×10^{-3} M) in iso-propanol (30 mL) onto the FTO substrates; Pt002, same procedure as Pt001 using H_2PtCl_6 (10^{-2} M) iso-propanol solution; Pt003, tape casting of Platisol paste (Solaronix); Pt004, tape casting of a viscous paste of 27 mg of potassium tetrachloroplatinate(II) (Aldrich) and 3.670 g of Polyethylene Glycol 20000 (PEG, Fluka) in 20 mL of H $_2$ O; Pt005, same procedure as Pt004 using 54 mg of potassium tetrachloroplatinate(II); Pt006, same procedure as Pt004 using 78.4 mg of potassium tetrachloroplatinate(II); Pt007, reference counter employing simple FTO glass.

All the electrodes were exposed to a thermal treatment in air at 500 °C for 30 min.

The electrodes were produced on the FTO substrate through the use of a pre-cut mask of Foto/Frasket film (Badger Co., U.S.A.).

The functionalization of the photoanodes was obtained by overnight adsorption of a (10^{-4} M) ethanol solution of *cis*-bis(thiocyano) ruthenium(II)-bis-2,2'-bipyridine-4,4'-dicarboxylate, [Ru(dcbpy) $_2$ (SCN) $_2$] [41].

The liquid electrolyte used was 0.3 M LiI, 0.03 M I $_2$, and 0.5 M *tert*-butylpyridine in CH $_3$ CN.

The realization of the gel electrolyte was obtained by mixing PMMA (molecular weight \sim 900,000), PC and CH $_3$ CN (Aldrich) [3].

The tests on new gel electrolyte recipes were conducted on small cells with a total area of 7.5 cm 2 and an active area of

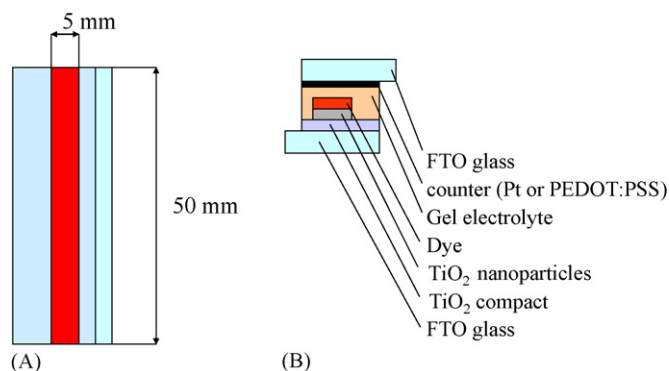


Fig. 1. Front view (A) and side view (B) of the cells with a real area of 7.5 cm^2 with an active area of 2.5 cm^2 .

2.5 cm^2 (Fig. 1). To evaluate the influence of a gel electrolyte, DSSCs were assembled using the same batch of counter electrodes and similar photoanodes obtained by absorbing the dye from the same absorption bath. This procedure gave photoanodes with similar absorption spectra ($50 \pm 1\%$ in transmittance at λ_{max} , 520 nm).

2.2. DSSCs testing

A solar simulator providing A.M. 1.5 illumination conditions (Solar Konstant 575 from Steuernagel (D)) was employed for all measurements under simulated sunlight. The spectral distribution and quality of the solar simulator was monitored using an AvaSpec 2048 spectrometer from Avantes and a Precision Pyranometer from Eppley Laboratories was used to monitor the total power that was set to the desired incident power. The electrical measurements were performed using Keithley 2400 Sourceme-ter providing short circuit current I_{sc} , voltage at open circuit V_{oc} , fill factor FF% and efficiency $\eta\%$ of the tested cells.

IV -curves were recorded in the interval $-2 \text{ V}/2 \text{ V}$ on the basis of the V_{oc} of the samples. Lifetime measurements under simulated sunlight were performed under short circuit conditions.

Autolab PGSTAT 10 was used for the measurements of the catalytic activity.

3. Results and discussion

3.1. TiO_2 substrate

Titania occurs naturally in three crystalline forms: rutile, anatase and brookite which have different band gap. Anatase has been studied intensively as a photocatalyst [42], and as dye supporting electron-transporting substrate [43].

The fundamental absorption, which corresponds to electron excitation from the valence band (VB) to the conduction band (CB), can be used to determine the nature and the value of the optical band gap. This can be obtained by a simple extrapolation of the absorption band edge or by the McLean analysis [44] which determines the band gap energy through the relation:

$$(\alpha h\nu)^n = A(h\nu - E_g)$$

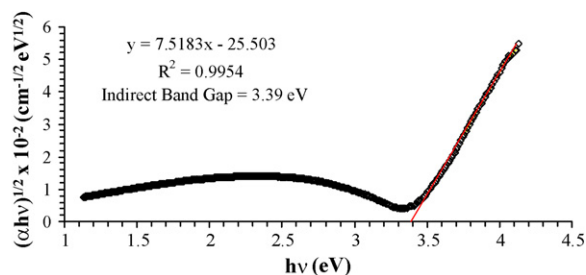


Fig. 2. TiO_2 anatase indirect allowed electron transition: band gap evaluation by linear fitting.

where A is a constant, E_g the band gap of the material, α is the absorption coefficient (cm^{-1}) and n depends on the type of electronic transition ($1/2$, $1/3$, 2 , $2/3$, for indirect allowed, indirect forbidden, direct allowed, direct forbidden). From the absorption spectrum of a spin coated layer of a compact film of TiO_2 on soda-lime glass [3] the optical band gap was evaluated to be 3.39 eV corresponding to the anatase phase of the oxide [45] (Fig. 2).

3.2. Pt counters

In testing the counter electrode contribution the same photoanode was used in temporarily sealed solar cells employing a liquid electrolyte. The absorption spectrum of the photoanode was controlled after every test in order to ensure that dye degradation was not taking place.

From Table 1 the best cell performance was obtained with the counter electrode Pt004 produced by the tape casting technique, which gave an efficiency of 0.4% under $100.7 \text{ mW}/\text{cm}^2$ due to the highest value of I_{sc} recorded. FF% was similar for all the samples apart from the FTO case (Pt007), where the high value of R_s gave a low FF% of 19.7% . The samples also showed a rectification around 1 between $-1/+1 \text{ V}$. In conclusion, the use of tape cast Pt samples gave cells with the best performance. The availability of a simple masking procedure of Pt electrode deposition that can follow the TiO_2 deposition, avoiding the air-brushing process, should also be considered as a great advantage for potential industrial production.

The tape cast Pt counter electrodes giving the best results were tested in a SC using a gel electrolyte with a conductivity of 9.2 mS cm^{-1} (G5, 0.7 g polymethyl-methacrylate, 2 g propylene carbonate, 1 M LiI and 0.1 M I_2) [3]. This gel has been chosen because a concentration of 0.1 M of I_2 allows transmittance in the visible region of more than 50% , while a higher concentration of LiI/I_2 redox couple induces a low transmittance in spite of increasing the conductivity (Fig. 3). Semi-transparency is crucial for application in transparent glazing surface. Modules produced by serially connected cells on the same FTO plate require balanced cells that can be illuminated from either side giving the same performances. IV characteristics of SCs, produced using G5, have shown analogous performance to the corresponding LCs (Fig. 4). In particular, a lower FF% resulted in a lower efficiency of the cell (0.25 and 0.24 as compared to 0.39 and 0.29 for the cells employing Pt004 and Pt005, respectively). Lifetime

Table 1
Photovoltaic performances of DSSCs using liquid electrolyte (active area 2 cm²) with different counter electrodes under standard illumination (100.7 mW/cm², A.M. 1.5, 25 °C).

Sample	I_{sc} (mA/cm ²)	V_{oc} (mV)	P_{max} (mW/cm ²)	FF%	$\eta\%$	R_s^a dark (Ω)	R_s light (Ω)	Diode factor
Pt001	0.58	575	0.145	43.5	0.14	95	112	1.2
Pt002	0.50	525	0.124	47.3	0.12	94	86	1.2
Pt003	0.29	575	0.080	47.8	0.08	88	105	1.4
Pt004	1.49	575	0.390	45.6	0.39	104	63	1.1
Pt005	0.91	625	0.289	50.9	0.29	75	62	1.0
Pt006	0.21	575	0.062	51.4	0.06	107	104	1.1
Pt007	0.20	525	0.021	19.7	0.02	256	213	1.0

^a Serial resistance (R_s) values were obtained by linear fitting of the I/V curves at voltage close to V_{oc} (0.7/1 V).

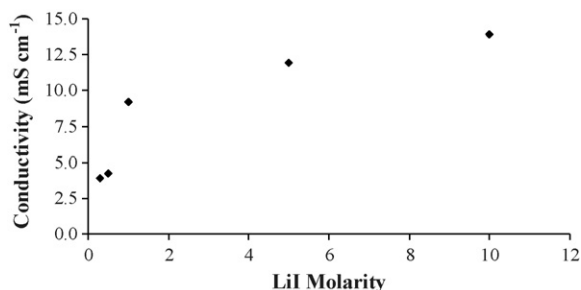


Fig. 3. Gel conductivities increase with the LiI/I₂ concentration in the gel.

tests have shown an increase in I_{sc} after few hours of irradiation, but a reduction in V_{oc} and FF% gave an overall performance decrease of the cell (Table 2).

From the lifetime test, the lowering of the R_{sh} after 40 h of irradiation is noticeable. This is an indication of a performance limiting factor at the photoanode, i.e. the presence of electron recombination processes at the TiO₂/dye interface. This could be due to the loss of CH₃CN, which is the most volatile solvent in the gel electrolyte, that cause depletion of I⁻ at the TiO₂/dye interface induced by lower mobility of I⁻ ions in a more viscous medium. The lower mobility prevents dye regeneration, increasing the electron recombination probability between the electron injected in the conduction band of the TiO₂ and the oxidized dye. After 40 h of irradiation an increase of R_s is observed. We ascribe this to the loss of Pt clusters at the counter electrode surface that can furthermore migrate to the photoanode and affect the efficiency of the charge transfer on the basis of previous unpublished results. The observed increase of R_s could also be due to a reduced conductivity of the gel electrolyte caused by CH₃CN loss.

Table 2
Photovoltaic performances of DSSCs with different counter electrodes employing a gel electrolyte assembly (G5) (active area 2.5 cm²) under standard illumination (100.7 mW/cm², A.M. 1.5, 25 °C)

Sample	I_{sc} (mA/cm ²)	V_{oc} (mV)	P_{max} (mW/cm ²)	FF%	$\eta\%$	R_s^a light (Ω)	R_{sh}^b light (Ω)	Diode factor
Pt004	1.23	525	0.251	38.9	0.25	69	379	1.1
Pt005	1.16	525	0.238	39.0	0.24	93	460	1.1
Pt005 ^c	0.22	275	0.025	40.6	0.02	134	275	1.1

^a Serial resistance (R_s) values were obtained by linear fitting of the I/V curves at voltage close to V_{oc} (0.7/1 V).

^b Shunt resistance (R_{sh}) values were obtained by linear fitting of the I/V characteristics at voltage close to 0 (−0.3/0 V).

^c Sample after 40 h of irradiation.

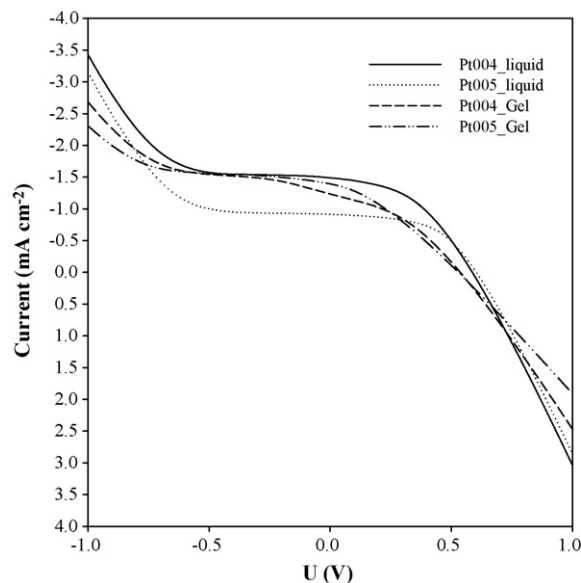


Fig. 4. Comparison between DSSC employing the two different counter electrodes Pt004 and Pt005 in liquid and gel electrolyte environment (G5).

The lifetime profile show an increase in I_{sc} during the first hours of irradiation [3], most probably due to an annealing process or to localized heating of the electrolyte followed by an exponential decrease that can be fitted by two exponential functions (Fig. 5).

3.3. Gel electrolytes

Gel electrolytes with different amounts of PC were tested in DSSCs under the same experimental condition (Table 3). The cell performances were similar in all cases (Table 4).

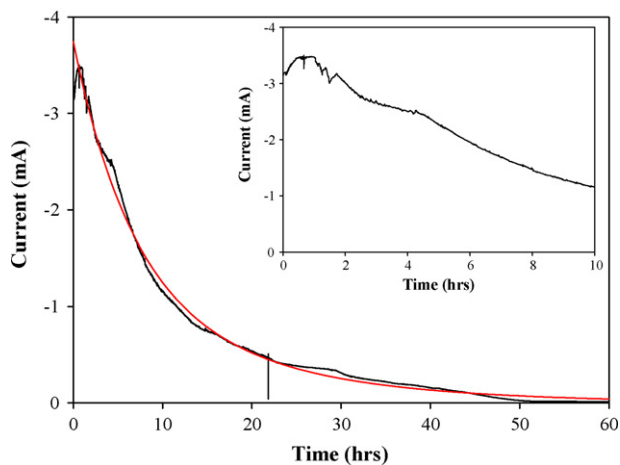


Fig. 5. Lifetime of DSSC employing Pt005 and the gel electrolyte G5. Inset: magnification of the first 10 h of irradiation. The indented behaviour was induced by variation of the sun simulator intensity.

Table 3
Gel electrolyte mixtures employing the same volume of CH₃CN (7 g)

Sample	PMMA (g)	PC (g)	LiI (M)	I ₂ (M)	Conductivities (mS cm ⁻¹) ^a
G12	0.7	4	0.5	0.05	5.88
G13	0.7	6	1	0.1	5.38
G14	1.4	6	1	0.1	4.16

^a The liquid electrolyte used gave a conductivity of 15.5 mS cm⁻¹.

Temporal decay of short circuit current in air was fitted using a bi-exponential decay according to literature [46]:

$$\frac{I_{sc}(t)}{I_{sc}(0)} = A e^{-bt} + C e^{-dt} \quad (1)$$

From the fitting the time constants (b , d) and the weighting of the individual exponential functions (A , C) for the two components can be obtained: $b = 2.4 \times 10^{-3} \text{ s}^{-1}$ and $d = 1.3 \times 10^{-3} \text{ s}^{-1}$, and, $b = 3.4 \times 10^{-3} \text{ s}^{-1}$ and $d = 1.8 \times 10^{-3} \text{ s}^{-1}$ for the cells with G12 and G5, respectively. We do not ascribe physical meaning to these parameters in the lifetime decay. This fit is simply and rather useful for a qualitative evaluation of the cell lifetime. The lower values of both components in the case of G12 indicate that the increase in lifetime moving from G5 to G12 was limited but indeed show the trend that a higher PC content corresponds to an increase in lifetime of the cell.

Therefore an increase in the high boiling point solvent content of the gel electrolyte, allows a longer lifetime leaving the PMMA

Table 4
Photovoltaic performances of DSSCs employing different gel electrolyte (active area 2.5 cm²) and Pt005 as counter electrode, under standard illumination (100.7 mW/cm², A.M. 1.5, 25 °C).

Sample	I_{sc} (mA/cm ²)	V_{oc} (mV)	P_{max} (mW/cm ²)	FF%	$\eta\%$	R_s^a light (Ω)	R_{sh}^b light (Ω)	Diode factor
G12	1.65	575	0.336	35.4	0.334	73	1153	1.2
G13	1.73	575	0.369	37.1	0.366	80	1305	1.1
G14	1.64	575	0.380	40.3	0.377	98	1836	1.2

^a Serial resistance (R_s) values were obtained by linear fitting of the I/V curves at voltage close to V_{oc} (0.7/1 V).

^b Shunt resistance (R_{sh}) values were obtained by linear fitting of the I/V characteristics at voltage close to 0 (−0.3/0 V).

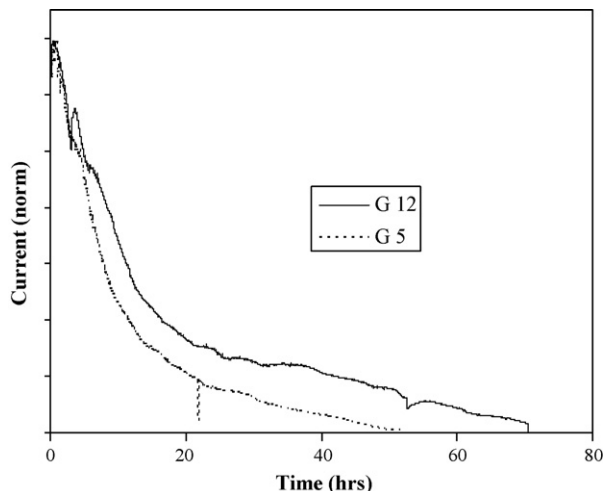


Fig. 6. Comparison of the lifetime of two DSSCs employing gel electrolyte G5 or G12.

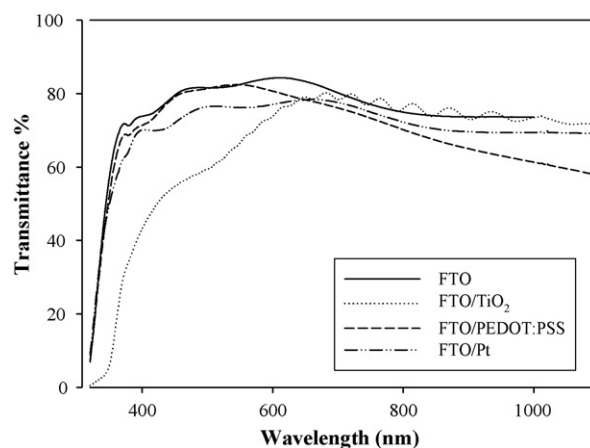


Fig. 7. Transmittance spectra showing the high transparency of the electrodes produced.

polymer matrix swollen with solvent thus preserving a good dye regeneration (Fig. 6).

3.4. PEDOT:PSS counter electrodes

Counter electrodes produced by spin coating a commercial solution of PEDOT:PSS preserved a high transparency in the visible region (Fig. 7). A thin layer of PEDOT:PSS reduces the transmittance of the cell mostly in the N.I.R. where the tested dyes do not absorb. In counter electrodes semi-transparency is,

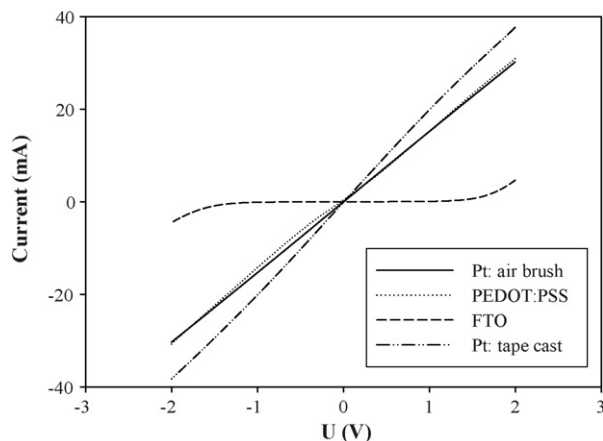


Fig. 8. Catalytic activities of four types of counter electrodes measured in a symmetric cell model electrode/gel electrolyte (G5)/model electrode.

once again, the key point for their use in serially connected elements in order to balance cells that are illuminated from the back [3].

Parallel plate thin layer cells, in which electrodes were separated by a 50 μm thick Surlin[®] film, were constructed to investigate the catalytic activities of the different counter electrodes used. *I/V* characteristics of cells with symmetric geometry (model electrode/electrolyte/model electrode) showed that tape cast Pt counter electrodes, in both gel and liquid electrolyte environment, have better catalytic activity than airbrushed Pt counter electrode (Figs. 8 and 9). PEDOT:PSS catalytic activity is comparable to airbrushed Pt using a gel electrolyte recipe with low PC content (G5) (Fig. 8) and with high PC content (G12) (not shown). Moreover, PEDOT:PSS catalytic activity is better in gel environment than in liquid environment.

We currently have no reasonable explanation for this but would suggest that the presence of gel electrolyte made it possible to realize a good physical contact between quasi-solid electrolyte and the smooth layer of PEDOT:PSS playing a role in the catalytic activity of the PEDOT:PSS quasi-solid-state solar cell [22].

The *I/V* characteristics of liquid (L) and gel (G5) constructions using three different dyes $\{(\text{C}_4\text{H}_9)_4\text{N}\}_4[\text{Ru}(\text{tcterpy})(\text{NCS})_3]$ (**1**) [47], $\{(\text{C}_4\text{H}_9)_4\text{N}\}_4[\text{Ru}(4\text{-}4'\text{dicarbossibpy})_2(\text{CN})_2]$ (**2**) [48] and $\{(\text{C}_4\text{H}_9)_4\text{N}\}_2[\text{Ru}(4\text{-}4'\text{dicarbossibpy})(\text{CN})_4]$ (**3**) [49] showed similar efficiency and confirmed the possibility of using PEDOT:PSS based counter electrodes in quasi-solid-state DSSC (Table 5).

Table 5
Photovoltaic performances of DSSCs employing gel (G5) and liquid electrolyte (L) assembly (active area 2.5 cm^2) for three different dyes (**1**, **2**, **3**) under standard illumination (100.7 mW/cm^2 , A.M. 1.5, 25 $^\circ\text{C}$).

Sample	I_{sc} (mA/cm^2)	V_{oc} (mV)	P_{max} (mW/cm^2)	FF%	$\eta\%$	R_s light ^a (Ω)
1 L	0.98	525	0.190	37.0	0.173	61
1 G5	1.01	528	0.203	38.0	0.186	86
2 L	1.99	602	0.343	28.6	0.315	75
2 G5	2.10	625	0.365	27.8	0.336	82
3 L	1.13	549	0.258	41.6	0.238	68
3 G5	1.20	525	0.246	39.1	0.226	57

^a Serial resistance (R_s) values were obtained by linear fitting of the *I/V* curves at voltage close to V_{oc} (0.7/1 V).

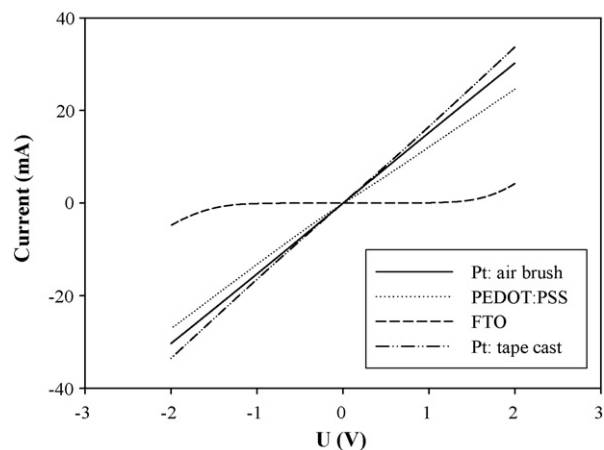


Fig. 9. Catalytic activities of four types of counter electrodes measured in a symmetric cell model electrode/liquid electrolyte/model electrode.

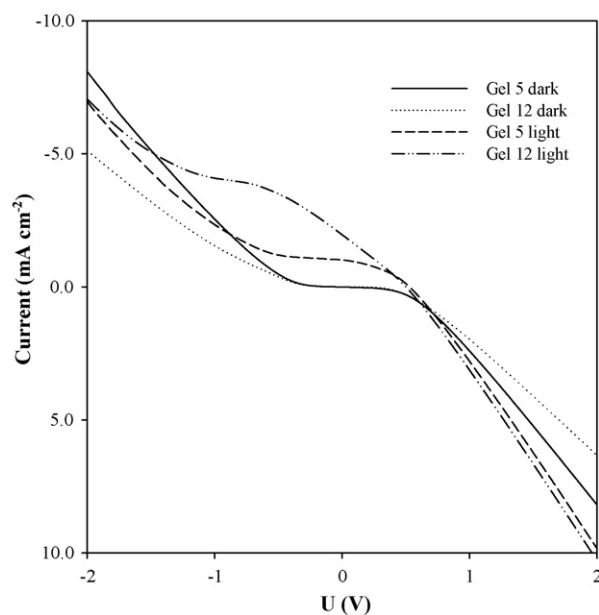


Fig. 10. *I/V* performance of DSSC using PEDOT:PSS as a counter electrode and two different gel recipe G5 and G12 with an higher content in PC.

In particular cell performances of SCs employing PEDOT:PSS as a counter electrode were better than the corresponding LCs, showing better photocurrents, in accordance with similar findings by Hayase and coworkers [22].

Quasi-solid-state DSSC sensitized by $\{(C_4H_9)_4N\}_4[Ru(tcterpy)(NCS)_3]$ employing gel electrolytes with different contents of PC (G5 and G12) were also tested using PEDOT:PSS as a counter electrode. Despite the low FF% the cells with this assembly have shown a I_{sc} of 2 mA/cm^2 and a V_{oc} of 501 mV under 100 mW cm^{-2} (Fig. 10).

4. Conclusion

The realization of highly transparent and stable solar cells is appealing for a future commercialization of such devices and complement highly efficient solar cells with poor transparency. We have demonstrated the possibility of producing highly transparent gel electrolyte solar cells with a performance similar to liquid electrolyte cells employing the same assembly.

Tape cast Pt counter electrodes have been produced and employed in SC assembly giving better performances than air-brushed electrodes. PEDOT:PSS have been shown to be an alternative to Pt based counter electrodes giving the best cell performance in SC assemblies. Finally, SC assemblies using gel electrolyte with a high content in PC have shown a longer lifetime, which is a prerequisite for any future application.

Acknowledgments

This work was supported by the Danish Technical Research Council FTP 274-05-0053. We would like to thank Dr. R. Argazzi for providing $\{(C_4H_9)_4N\}_2[Ru(4-4'\text{-dicarbossibpy})(CN)_4]$.

References

- [1] B. O'Regan, M. Grätzel, *Nature* 353 (1991) 737.
- [2] M. Grätzel, *Nature* 414 (2001) 338.
- [3] M. Biancardo, K. West, F.C. Krebs, *Sol. Energy Mater. Sol. Cells* 90 (2006) 2575.
- [4] K. Tennakone, G.R.A. Kumara, A.R. Kumarasinghe, K.G.U. Wijayantha, P.M. Sirimanne, *Semicond. Sci. Technol.* 10 (1995) 1689.
- [5] B. O'Regan, F. Lenzmann, R. Muis, J. Wienke, *Chem. Mater.* 14 (2002) 5023.
- [6] J. Kruger, R. Plass, M. Grätzel, H.J. Matthieu, *Appl. Phys. Lett.* 81 (2002) 367.
- [7] N. Papageorgiou, Y. Athanassov, M. Armand, P. Bonhote, H. Pettersson, A. Azam, M. Grätzel, *J. Electrochem. Soc.* 143 (1996) 3099.
- [8] H. Paulsson, A. Hagfeldt, L. Kloo, *J. Phys. Chem. B* 107 (2003) 13665.
- [9] P. Wang, S.M. Zakeeruddin, J.-E. Moser, R. Humphry-Baker, M. Grätzel, *J. Am. Chem. Soc.* 126 (2003) 7164.
- [10] H. Lindström, A. Holberg, E. Magnusson, L. Malmqvist, A. Hagfeldt, *J. Photochem. Photobiol. A: Chem.* 145 (2001) 107.
- [11] F. Cao, G. Oskam, P.C. Searson, *J. Phys. Chem.* 99 (1995) 17071.
- [12] W. Kubo, K. Murakoshi, T. Kitamura, S. Yoshida, M. Hakuri, K. Hanabusa, H. Shirai, Y. Wada, S. Yanagida, *J. Phys. Chem. B* 105 (2001) 12809.
- [13] W. Kubo, T. Kitamura, K. Hanabusa, Y. Wada, S. Yanagida, *Chem. Commun.* (2002) 374.
- [14] W. Kubo, S. Kambe, S. Nakade, T. Kitamura, K. Hanabusa, Y. Wada, S. Yanagida, *J. Phys. Chem. B* 107 (2003) 4374.
- [15] P. Wang, S. Zakeeruddin, J.E. Moser, M.K. Nazeeruddin, T. Sekigushi, M. Grätzel, *Nat. Mater.* 20 (2003) 402.
- [16] P. Wang, S.M. Zakeeruddin, P. Comte, I. Exnar, M. Grätzel, *J. Am. Chem. Soc.* 125 (2003) 1166.
- [17] A.F. Nogueira, M.-A. De Paoli, *Sol. Energy Mater. Solar Cells* 61 (2000) 135.
- [18] A.F. Nogueira, J.R. Durrant, M.-A. De Paoli, *Adv. Mater.* 13 (2001) 826.
- [19] T. Stergiopoulos, I.M. Arabatzis, G. Katsaros, P. Falaras, *Nanoletters* 2 (2002) 1259.
- [20] T. Yohannes, O. Inganäs, *Sol. Energy Mater. Solar Cells* 51 (1998) 193.
- [21] Y. Saito, T. Kitamura, Y. Wada, S. Yanagida, *Chem. Lett.* (2002) 1060.
- [22] Y. Shibata, T. Kato, T. Kado, R. Shiratuchi, W. Takashima, K. Kaneto, S. Hayase, *Chem. Commun.* (2003) 2730.
- [23] Y. Saito, W. Kubo, T. Kitamura, Y. Wada, S. Yanagida, *J. Photochem. Photobiol. A: Chem.* 164 (2004) 153.
- [24] A.F. Nogueira, C. Longo, M.A. De Paoli, *Coord. Chem. Rev.* 248 (2004) 1455.
- [25] K.M. Abraham, in: B. Scrosati (Ed.), *Application of Electroactive Polymer*, Chapman & Hall, London, 1993.
- [26] J.Y. Song, Y.Y. Wang, C.C. Wan, *J. Power Sources* 77 (1999) 183.
- [27] J.L. Acosta, E. Morales, *J. Appl. Polym. Sci.* 60 (1996) 1185.
- [28] M. Cowie, in: J.R. MacCallum, C.A. Vincent (Eds.), *Polymer Electrolyte Reviews-1*, Elsevier, London, 1987.
- [29] O. Bohnke, C. Rousselot, P.A. Gillet, C. Truche, *J. Electrochem. Soc.* 139 (1992) 1862.
- [30] A.G. Bayer, European Patent 339,340 (1988).
- [31] Y. Saito, N. Fukuri, R. Senadeera, T. Kitamura, Y. Wada, S. Yanagida, *Electrochem. Commun.* 6 (2004) 71.
- [32] N. Fukuri, Y. Saito, W. Kubo, R. Senadeera, T. Kitamura, Y. Wada, S. Yanagida, *J. Electrochem. Soc.* 151 (2004) A1745.
- [33] Y. Saito, T. Azechi, T. Kitamura, Y. Hasegawa, Y. Wada, S. Yanagida, *Coord. Chem. Rev.* 248 (2004) 1469.
- [34] F.O. Lenzmann, B.C. O'Regan, J.J.T. Smits, H.P.C.E. Kuipers, P.M. Sommeling, L.H. Slooff, J.A.M. van Roosmalen, *Prog. Photovolt.: Res. Appl.* 13 (2005) 333.
- [35] A. Hauch, A. Georg, *Electrochim. Acta* 46 (2001) 3457.
- [36] N. Papageorgiou, *Coord. Chem. Rev.* 248 (2004) 1421.
- [37] W.B. Wang, B. Wei, Z. Luo, X.R. Xiao, Y. Lin, *Chin. J. Chem.* 22 (2004) 256.
- [38] M. Späth, P.M. Sommeling, J.A.M. van Roosmalen, H.J.P. Smit, N.P.G. van der Burg, D.R. Mahieu, N.J. Bakker, J.M. Kroon, *Prog. Photovolt.* 11 (2003) 207.
- [39] G. Khelashvili, S. Behrens, C. Weidenthaler, C. Vetter, A. Hirsch, R. Kern, K. Skupien, E. Dinjus, H. Bönemann, *Thin Solid Films* 511–512 (2006) 342.
- [40] L. Bay, K. West, B. Wither-Jensen, T. Jacobsen, *Sol. Energy Mater. Sol. Cells* 90 (2006) 341.
- [41] M.K. Nazeeruddin, A. Kay, I. Rodicio, R. Humphry-Baker, E. Muller, P. Liska, N. Vlachopoulos, M. Grätzel, *J. Am. Chem. Soc.* 115 (1993) 6382.
- [42] L. Cassar, *MRS Bull.* 29 (2004) 328.
- [43] A. Hagfeldt, M. Grätzel, *Acc. Chem. Res.* 33 (2000) 269.
- [44] T.P. McLean, *Prog. Semicond.* 5 (1960) 55.
- [45] H. Tang, F. Lévy, H. Gerger, P.E. Schmid, *Phys. Rev. B* 52 (1995) 7771.
- [46] F.C. Krebs, J.E. Carlé, N. Cruys-Bagger, M. Andersen, M.R. Lilliedal, M.A. Hammond, S. Hvidt, *Sol. Energy Mater. Sol. Cells* 86 (2005) 499.
- [47] M.K. Nazeeruddin, P. Péchy, T. Renouard, S.M. Zakeeruddin, R. Humphry-Baker, P. Comte, P. Liska, L. Cevey, E. Costa, V. Shklover, L. Spiccia, G.B. Deacon, C.A. Bignozzi, M. Grätzel, *J. Am. Chem. Soc.* 123 (2001) 1613.
- [48] T.A. Heimer, C.A. Bignozzi, G.J. Meyer, *J. Phys. Chem.* 97 (1993) 11987.
- [49] Received from Dr. R. Argazzi.